Strain energy and electronic structures of silicon carbide nanotubes: Density functional calculations

Mingwen Zhao,[1,*] Yueyuan Xia,[1] Feng Li,[1] R. Q. Zhang,[2] and S.-T. Lee[2]
[1]*Department of Physics, Shandong University, Jinan 250100, Shandong, China*
[2]*Centre of Super-Diamond and Advanced Films (COSDAF) & Department of Physics and Materials Science, City University of Hong Kong, Hong Kong SAR, China*
(Received 5 July 2004; revised manuscript received 15 November 2004; published 15 February 2005)

We perform density functional calculations for the geometrics, strain energy, and electronic structures of silicon carbide nanotubes (SiCNT's). We find that the strain energy in SiCNT's is as higher as 0.686 eV/atom relative to 3C-SiC for (5,5) SiCNT and decreases with increasing tube diameter. All the SiCNT's are semiconductors, the band gap of which increases with increasing tube diameter. In contrast to 3C-SiC, zigzag SiCNT has a direct band gap at the Γ point, whereas armchair and chiral tubes have an indirect band gap. The highest occupied valance band and the lowest unoccupied conduction band highly localize to C and Si atoms, respectively. Hydrogen-decorated SiCNT's display the characters of *p*- or *n*-type semiconductors depending on the adsorbing site.

DOI: 10.1103/PhysRevB.71.085312 PACS number(s): 72.80.Rj, 73.20.At, 61.46.+w

INTRODUCTION

Since the discovery of carbon nanotubes,[1] the fabrication of nanometer-scaled one-dimensional materials has attracted considerable attention because of their potential use in both nanotechnology and nanoscale engineering. Due to quantum-size effects, one-dimensional nanostructures possess unique properties compared to corresponding bulk materials. For example, the electronic structure of carbon nanotubes (CNT's) can be either metallic or semiconducting depending on their chiral vectors (n,m).[2–4] The energy gap of silicon nanowires (SiNW's) was found to increase with decreasing wire diameter from 1.1 eV for 7 nm to 3.5 eV for 1.3 nm,[5] and a transition from an indirect to direct band gap was predicted to occur as the diameter is smaller than 0.77 nm.[6] ZnO with diverse nanostructures, such as nanowires, nanoribbons, nanohelixes, nanotubes, and nanocages, is another unique material that exhibits a large exciton binding energy (60 meV), a wide band gap (3.37 eV), and a low lasing threshold and thus has potential applications in optoelectronics, sensors, transducers, and biomedical sciences.[7] It has also been revealed that tubular structures of III–V compounds, such as BN, AlN, and GaN, display the characters of band structure quite different from their bulk materials. For example, zigzag tubes are direct band-gap semiconductors, whereas armchair tubes have an indirect band gap.[8–10] The existence of a direct band gap in zigzag group-III nitride nanotubes is important, because it indicates that such nanostructures may exhibit strong electroluminescence, which has never been observed for their bulk materials. Considerable efforts have therefore been made to synthesize nanosized structures, such as silicon carbide nanowires,[11,12] gallium nitride nanowires,[13] Si-B-C-N nanorodes,[14] heterostructures of carbon nanotubes, and carbide nanorode.[15]

Among the various semiconducting materials, silicon carbide (SiC) possesses unique physical and electronic properties, which make it a suitable material for electronic devices for high-temperature, high-power, and high-frequency applications.[16] Recently, one-dimensional silicon carbide nanotubes (SiCNT's) and nanowires of various shapes and structures were synthesized via the reaction of silicon (produced by disproportionation reaction of SiO) with multiwalled CNT's (as templates) at different temperatures.[17] The produced multiwalled SiCNT's have interlayer spacings ranging from 3.8 Å to 4.5 Å, significantly larger than 3.4 Å normally observed for the multiwalled CNT's. The energetically favorable configuration was predicted to consist of alternating Si and C atoms with each Si (or C) atom having as nearest neighbors only C (or Si) atoms and vice versa, on the basis of the generalized tight-binding molecular-dynamics and *ab initio* calculations.[18,19] SiCNT's are expected to have the advantages over CNT's because they may possess high reactivity of exterior surface facilitating to sidewall decoration and stability at high-temperature. The stability of SiCNT's against oxidation in air may exceed 1000 °C, which would enable high-temperature, harsh-environment nanofiber- and nanotube-reinforced ceramics. Experimentally, the transformation of SiCNT to 3C-SiC (zinc-blended) structure was also observed under an electron beam annealing at the energy of 200 kV.[17] This result indicates that the SiCNT structure maybe an intermediate-metastable phase in the reaction between carbon nanotubes and silicon to form 3C-SiC nanowires. However, no theoretical support has been provided so far. The strain energy in SiCNT's relative to their bulk materials is helpful for evaluating the stability of SiCNT's and therefore is worth investigating. Moreover, SiCNT's are expected to have electronic properties quite different from their bulk materials and CNT's. To our knowledge, studies of the dependence of electronic structures on the chirality and diameter of SiCNT's are scarce and are therefore highly desirable.

THEORETICAL APPROACHES AND COMPUTATIONS

We performed density functional (DF) calculations using an efficient *ab initio* code, known as SIESTA.[20–22] This code is

based on density functional theory adopting a localized linear combination of numerical atomic-orbital basis sets for the description of valance electrons and norm-conserving nonlocal pseudopotentials for the atomic core. The pseudopotentials were constructed using the Trouiller-Martins scheme[23] to describe the valance electron interaction with the atomic core; the nonlocal components of the pseudopotential were expressed in the fully separable form of Kleiman and Bylander.[24,25] The Perdew-Burke-Ernzerhof (PBE) form generalized gradient approximation (GGA) corrections were used for the exchange-correlation potential.[26] The atomic orbital basis set employed throughout was a double-ζ plus polarization (DZP) function. The charge density was projected on a real space grid with an equivalent cutoff 100 Ry to calculate the self-consistent Hamiltonian matrix elements. The periodic boundary condition along the tube axis was employed for SiCNT's with a vacuum region (10 Å) between tubes to make sure that there is no interaction between SiCNT's. The supercells of the armchair and zigzag SiCNT's contain eight layers of atoms along the tube axis. In order to determine the equilibrium configurations of SiCNT's under study, we relaxed all the atomic coordinates together with the supercells using a conjugate gradient (CG) algorithm, until each component of the stress tensor was below 0.5 GPa and the atomic forces <0.02 eV/Å. In the calculations of the total energies and band structures, according to the Monkhorst-Pack approximation,[27] we used 8 (chiral tubes) and 32 (armchair and zigzag tubes) k points along the tube axis.[28] Binding energies were calculated from the difference between the total energy of SiCNT's and the energies of the corresponding isolated Si and C atoms.

RESULTS AND DISCUSSION

We first obtained the equilibrium configurations of SiCNT's with different diameters and chiralities, where Si and C atoms are placed alternatively without any adjacent Si or C atoms. The equilibrium configurations of (5,5), (8,0), and (9,3) SiCNT's are shown in Fig. 1. The average Si-C bond length of these tubes is about 1.80 Å in our calculations, in good agreement with other *ab initio* results,[18] slighter shorter than that of 3C-SiC structure, 1.89 Å.[29] Due to the slight difference in hybridization of Si and C atoms on the curved hexagonal layers, Si atoms moved toward the tube axis and C atoms moved in the opposite direction after relaxation, resulting in a buckling structure. The radial buckling was 0.096 Å for (5,5) tube and 0.089 Å for (9,0) tubes. The larger the diameter the slighter the buckling will be. For (11,11) tubes, the buckling is only 0.042 Å. This reconstruction is similar to the results observed for group-III nitride nanotubes where N atoms rotate outward and group-III atoms move inward.[9,10,30] The surface dipoles resulted from these bucklings may be relevant for potential applications in piezoelectricity of these tubes. The binding energy of (5,5) SiCNT is calculated to be about −7.54 eV/atom on the basis of the equilibrium configuration.

We then calculated the binding energy of 3C-SiC. We chose a cubic supercell of 64 atoms for 3C-SiC. Periodical boundary conditions were applied along x, y, and z directions. The lattice was relaxed together with the atomic coordinates in the CG minimization until the stress tolerance was less than 0.5 GPa and force tolerance less than 0.02 eV/atom. The optimized binding energy was −6.854 eV/atom, with the nearest-neighbor distance of 1.91 Å or equivalently the cubic lattice constant of 4.41 Å, in good agreement with the experimental results[29] and other DF calculations.[31,32] The strain energy involved in SiCNT's relative to 3C-SiC can therefore be determined from the difference between the binding energy of SiCNT's and that of 3C-SiC materials. Figure 2 plots the variation of strain energy involved in different SiCNT's as a function of tube diameter. It is obvious that the strain energy decreases with increasing tube diameter. The strain energy involved in (5,5) SiCNT relative to cubic SiC material is about 0.686 eV/atom from our calculations. For (11,11) SiCNT,

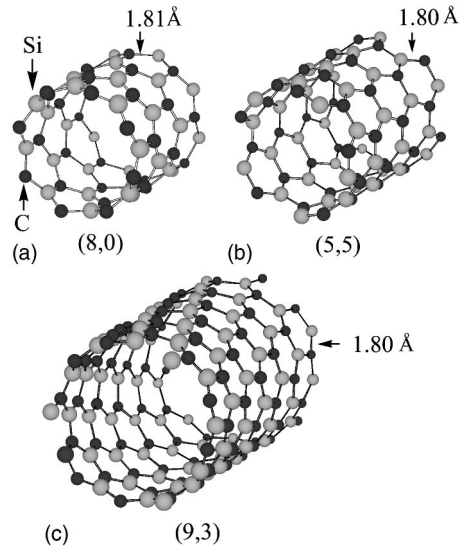

FIG. 1. Optimized supercells of (a) (8,0), (b) (5,5), and (9,3) SiCNT's. Gray and black balls represent silicon and carbon atoms, respectively. The diameters of these tubes are 8.01 Å for (8,0), 8.64 Å for (5,5), and 10.77 Å for (9,3) SiCNT's.

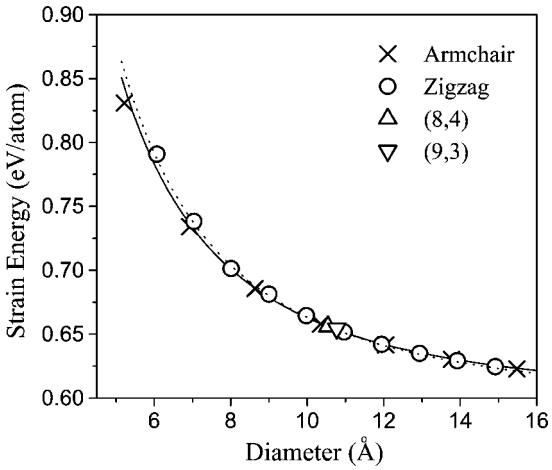

FIG. 2. Variation of strain energy (E_s) in SiCNT's relative to 3C-SiC with tube diameter (D). The solid and dotted lines are the fit to $E_s = E_0 + \alpha/D^2$ (see text).

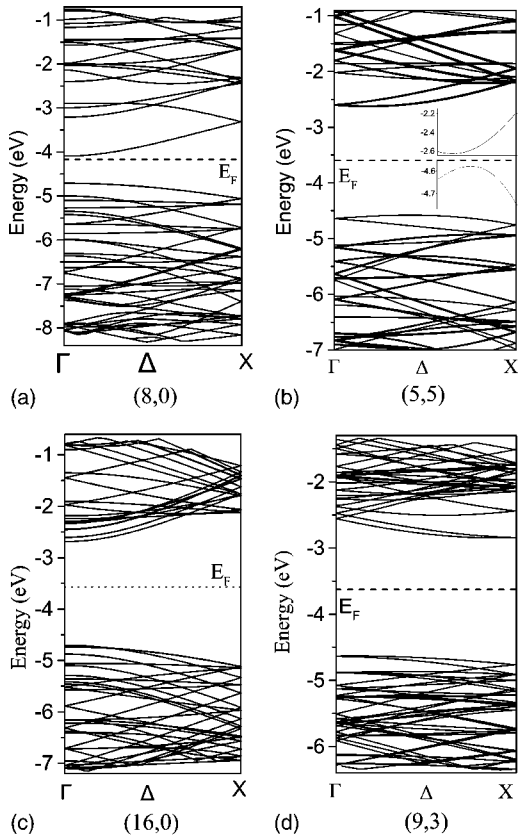

FIG. 3. Band structures along the tube axis of (a) (8,0), (b) (5,5), (c) (16,0), and (d) (9,3) SiCNT's. The Fermi levels (E_F) of these tubes are denoted by the dashed lines in the figure.

the strain energy decreases to 0.613 eV/atom. These strain energies are relatively high, indicating SiCNT's are a metastable phase and likely to transform to cubic structures, such as 3C-SiC nanowires, under certain conditions. We also find that the strain energy in SiCNT's is approximately proportional to the inverse square of the tube diameter. The variation of strain energy E_s as a function of tube diameter D can be fitted to the data given by the expression $E_s = E_0 + \alpha/D^2$, where E_0 corresponds to the strain energy involved in graphitic sheet of SiC. The fitting parameters of E_0 and α are calculated to be 0.595 eV and 6.78 eV Å^2 for armchair and 0.591 eV and 7.22 eV Å^2 for zigzag SiCNT's. This suggests that SiCNT's follow classical elasticity theory. Similar to the results of BN,[8] AlN,[9] and GaN,[10] the strain energy in SiCNT's is relatively insensitive to the chirality of the tube, but in contrast to the fact that carbon armchair nanotubes are more stable than zigzag nanotubes.[33]

We calculated the electronic structure of (8,0), (5,5), (16,0), and (9,3) SiCNT's, utilizing the nonlocal DF calculations in the generalized approximation. The diameters of these tubes are 8.01, 8.64, 15.9, and 10.77 Å, respectively. The length of the unit cells (L) of these SiCNT's along the tube axis are 12.64 Å for (5,5), 10.78 Å for (8,0) and (16,0), and 19.43 Å for (9.3). The calculated electron energy bands of these tubes are presented in Fig. 3. Unlike the character of carbon nanotubes that armchair is metallic, all of these SiCNT's are semiconductors with the band gap ranging from

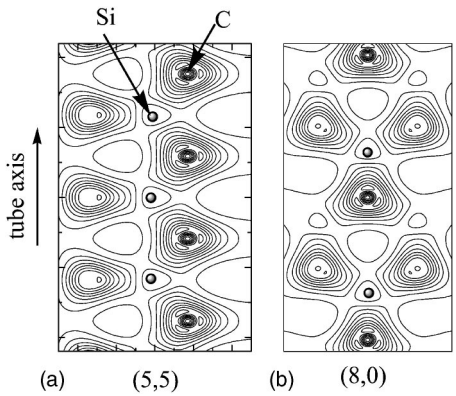

FIG. 4. Total valance charge density contours in the tangent planes of (a) (5,5) and (b) (8,0) SiCNT's. The solid circles indicate the positions of Si atoms.

0.90 to 1.83 eV.[34] This is related to the higher ionicity of SiC leading to the opening of a band gap in the hexagonal structure compared to semimetallic graphite. This result also accords with the features of the valance charge distribution in SiCNT's (as shown in Fig. 4). Because of strong 2p potential of the C atom, the valance charge density is strongly accumulated around the C atom, resulting in large asymmetry in charge distribution, displaying features of typical ionic bindings. The charge transfer from Si to C is about $0.45|e|$ for (4,4) SiCNT as revealed from the analysis of Mulliken population, close to the value $0.6|e|$ obtained by using other *ab initio* calculations.[19] Connecting the asymmetry of the charge density to the ionicity of a compound, Carcia and Cohen predicted that cubic SiC has an ionicity similar to many III–V materials.[35] Therefore, it is not surprising that SiCNT's possess characteristic energy bands similar to BN,[8] AlN,[9] and GaN[10] nanotubes.

3C-SiC material has been revealed to possess an indirect band gap of about 2.4 eV in previous literature.[30,31] Therefore, it is interesting to compare the differences in the band structures of armchair and zigzag nanotubes. Our calculations show that armchair and chiral SiCNT's have an indirect band gap similar to 3C-SiC, whereas zigzag SiCNT's have a direct band gap (Γ-Γ). The top of the HOVB in (5,5) SiCNT is at about $0.43(0,0,1)\pi/L$, while the bottom of the LUCB is at $0.18(0,0,1)\pi/L$. For (9,3) SiCNT, the top of the HOVB and the bottom of the LUCB are at the Γ and X points, respectively. The existence of a direct band gap in zigzag nanotubes is significant, since it suggests that such nanostructures may exhibit strong electroluminescence, which has never been observed for their bulk materials.[36]

We also investigated the diameter dependence of band gap for armchair, zigzag, and chiral SiCNT's. The evolution of the band gaps of these tubes as a function of diameter is plotted in Fig. 5. Quite different from the features of carbon nanotubes that armchair tubes are all metallic, whereas zigzag tubes oscillate between the metals and small- to medium-gap semiconductors, the calculated band gap of SiCNT's increases monotonically with increasing diameter and saturates at the calculated gap for graphitic sheet of SiC. This is similar to the results of BN,[8] AlN,[9] and GaN[10] nanotubes, and may be related to the curvature-induced σ-π hybridization in

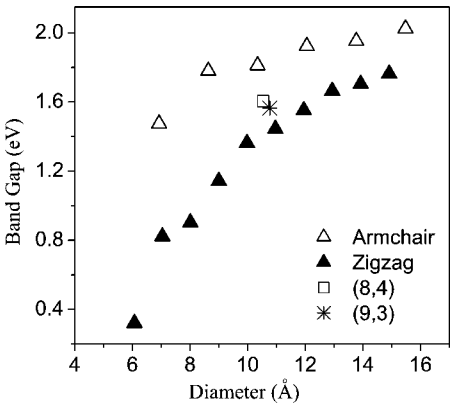

FIG. 5. Dependence of band gap of armchair (open uptriangles), zigzag (solid uptriangles), and chiral (open square and star) SiCNT's as a function of the tube diameter.

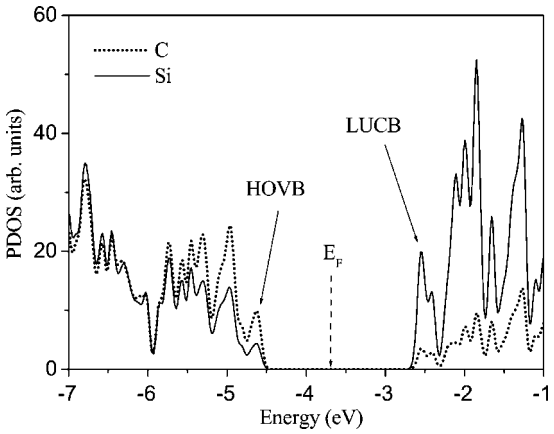

FIG. 6. PDOS of (5,5) SiCNT projected to Si (solid line) and C (dotted line), respectively. The energy at Fermi level is denoted by the dashed arrow in this figure.

SiCNT's with different diameters. It was already pointed out that rehybridization in small nanotubes shifts the π^* and σ^* bands to lower and higher energies, respectively.[37,38] The energy of LUCB at the Γ point for (8,0) SiCNT is downshifted by 1.41 eV compared to that in (16,0) SiCNT, whereas no remarkable change observed for HOVB, reducing the band gap of (8,0) tube to 0.9 eV [as shown in Figs. 3(a) and 3(c)]. As the diameter of SiCNT becomes larger, the band gap increases due to the repulsion between π and π^* states. We can also see from Fig. 5 that for the SiCNT's with similar diameters, (6,6), (11,0), and (8,4) tubes, the armchair tube has a larger band gap than the zigzag tube at about 0.4 eV, while the band gap of chiral SiCNT is in the middle. These

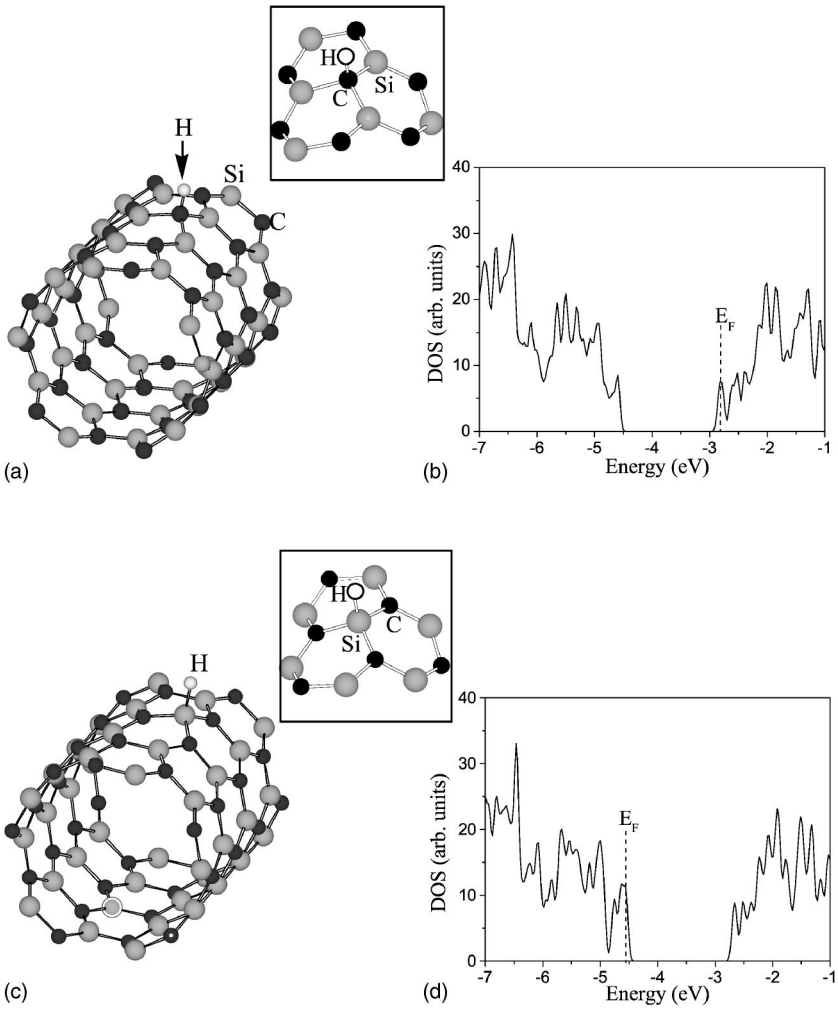

FIG. 7. Optimized supercells and DOS of H-decorated (5,5) SiCNT. The H atom chemically adsorbs above a C [(a) and (b)] and Si [(c) and (d)] on the tube wall. The Fermi levels (E_F) are indicated by the dashed lines. The local maps near the adsorbing sites are also presented as the insets of this figure.

results imply that the curvature-induced σ-π hybridization has the most pronounced effect on zigzag SiCNT's, resulting in a strong downshift of the conduction bands, whereas the electronic band structure of armchair and chiral tubes is less affected.

Finally, we present the density of states projected to different atoms (PDOS) of (5,5) SiCNT in Fig. 6. From this figure, it is obvious that the HOVB and LUCB are highly localized to C and Si atoms, separately. This is coincident with the results that the valance charge density is strongly accumulated around C atoms (as shown in Fig. 4). This asymmetry suggests that sidewall decoration of SiCNT's with the same atom or radical at different site (C or Si atom) on the tube wall may result in different electronic properties. As a test, we calculated the density of states (DOS) of hydrogen-decorated (5,5) SiCNT, where an H atom adsorbs at the C and Si atoms, respectively (as shown in Fig. 7). When an H atom chemically adsorbs above a C atom at the exterior of the tube [Fig. 7(a)], the hybridization of the C atom changes from sp^2 to sp^3, breaking the related π-π bonds nearby and resulting in a local state close to the LUCB [Fig. 7(b)]. Further analysis shows that this local state mainly arises from the states of the three Si atoms nearest to the C atom. This local state is half-occupied and therefore acts as a donor state, making the hydrogen-decorated SiCNT display the characters of *n*-type semiconductors. When an H atom adsorbs above a Si atom [Fig. 7(c)], things are quite different, however. A local state that mainly localizes to the C atoms nearest to the Si atom appears close to the HOVB caused by the decoration of H atom. This half-occupied local state can therefore act as an acceptor state, making the hydrogen-decorated SiCNT have the characters of *p*-type semiconductors. In view of the higher reactivity of exterior surface of SiCNT's in facilitating sidewall decoration, this result is rather important since different types of semiconductors can be obtained through chemical decoration with the same radical at different sites (C or Si atom).

CONCLUSION

Our calculations show that the strain energy involved in SiCNT's relative to 3C-SiC can be as higher as 0.686 eV/atom for (5,5) SiCNT and decreases with increasing tube diameter. All the SiCNT's are semiconductors with the band gap depending on the diameter and chirality. Armchair and chiral SiCNT's are indirect band gaps, whereas the zigzag tube has a direct band gap at the Γ point. The band gap increases with increasing tube diameter. The HOVB and LUCB mainly localize at the C and Si atoms, separately. Hydrogen-decorated SiCNT's display the characters of *p*- or *n*-type semiconductors depending on the H-adsorbing site.

ACKNOWLEDGMENTS

This work is supported by the National Natural Science Foundation of China under Grant Nos. 50402017, 10374059, and 90203013, and by a CityU Strategic Grant (Project No. 7001390). R.Q.Z. and S.T.L. acknowledge the support from CAS-Croucher Funding Scheme for Joint Laboratories and Chinese Academy of Sciences, China. All the calculations were performed in the Centre of High Performance Computation of Shandong Province.

*Author to whom correspondence should be addressed. Electronic address: zmw@sdu.edu.cn

[1] S. Iijima, Nature (London) **354**, 56 (1991).
[2] J. W. Mintmire, B. I. Dunlap, and C. T. White, Phys. Rev. Lett. **68**, 631 (1992).
[3] N. Hamada, S. I. Sawada, and A. Oshiyama, Phys. Rev. Lett. **68**, 1579 (1992).
[4] R. Saito, M. Fujita, G. Dresselhaus, and M. S Dresselhaus, Appl. Phys. Lett. **60**, 2204 (1992).
[5] D. D. D. Ma, C. S. Lee, F. C. K. Au, S. Y. Tong, and S. T. Lee, Science **299**, 1874 (2003).
[6] J. B. Xia and K. W. Cheah, Phys. Rev. B **55**, 15 688 (1997).
[7] Z. L. Wang, Mater. Today **7** (6), 26 (2004) and references therein.
[8] A. Rubio, J. L. Corkill, and M. L. Cohen, Phys. Rev. B **49**, 5081 (1994).
[9] M. W. Zhao, Y. Y. Xia, D. J. Zhang, and L. M. Mei, Phys. Rev. B **68**, 235415 (2003).
[10] S. M. Lee, Y. H. Lee, Y. G. Hwang, J. Elsner, D. Porezag, and Th. Frauenheim, Phys. Rev. B **60**, 7788 (1999).
[11] H. J. Dai, E. W. Wong, Y. Z. Lu, S. S. Fan, and C. M. Lieber, Nature (London) **375**, 769 (1995).
[12] Z. Pan, H. L. Lai, F. C. K. Au, X. F. Duan, W. Y. Zhou, W. S. Shi, N. Wang, C. S. Lee, N. B. Wang, S. T. Lee, and S. S. Xie, Adv. Mater. (Weinheim, Ger.) **12**, 1186 (2000).
[13] W. Q. Han, S. S. Fan, Q. Q. Li, and Y. D. Hu, Science **277**, 1287 (1997).
[14] Y. Zhang, K. Suenaga, C. Colliex, and S. Iijima, Science **281**, 973 (1998).
[15] Y. Zhang, T. Ichihashi, E. Landree, F. Nihey, and S. Iijima, Science **285**, 1719 (1999).
[16] *Properties of Silicon Carbide*, edited by G. L. Harris (INSPEC, Institution of Electrical Engineers, London, 1995).
[17] X. H. Sun, C. P. Li, W. K. Wong, N. B. Wong, C. S. Lee, S. T. Lee, and B. T. Teo, J. Am. Chem. Soc. **124**, 14 464 (2002).
[18] M. Menon, E. Richter, A. Mavrandonakis, G. Froudakis, and A. N. Andriotis, Phys. Rev. B **69**, 115322 (2004).
[19] A. Mavrandonakis, G. E. Froudakis, M. Schnell, and M. Muhlhăuser, Nano Lett. **3**, 1481 (2004).
[20] P. Ordejón, E. Artacho, and J. M. Soler, Phys. Rev. B **53**, R10 441 (1996).
[21] D. Sánchez-Portal, P. Ordejón, E. Artacho, and J. M. Soler, Int. J. Quantum Chem. **65**, 453 (1997).
[22] J. M. Soler, E. Artacho, J. D. Gale, A. García, J. Junquera, P. Ordejón, and D. Sánchez-Portal, J. Phys.: Condens. Matter **14**, 2745 (2002) and references therein.
[23] N. Troullier and J. L. Martins, Phys. Rev. B **43**, 1993 (1991).
[24] L. Kleinman and D. M. Bylander, Phys. Rev. Lett. **48**, 1425 (1982).

[25] D. M. Bylander and L. Kleinman, Phys. Rev. B **41**, 907 (1990).
[26] J. P. Perdew, K. Burke, and M. Ernzerhof, Phys. Rev. Lett. **77**, 3865 (1996); **78**, 1396(E) (1997).
[27] H. J. Monkhorst and J. D. Pack, Phys. Rev. B **13**, 5188 (1976).
[28] In principle, the longer the supercell, the fewer *k* points are needed to obtain stable results of energetics and band structures. We increased the number of *k* points based on those selected in the present calculations and found no differences worth mentioning.
[29] *Physics of Group IV Elements and III–V Compounds*, edited by O. Madelung, Landolt-Börnstein, New Series, Group III, Vol. 17a (Springer, Berlin, 1982).
[30] M. Menon and D. Srivastava, Chem. Phys. Lett. **307**, 407 (1999).
[31] C. Persson and U. Lindefelt, J. Appl. Phys. **82**, 5496 (1997).
[32] C. H. Park, B. H. Cheong, K. H. Lee, and K. J. Chang, Phys. Rev. B **49**, 4485 (1994).
[33] D.-H. Oh and Y. H. Lee, Phys. Rev. B **58**, 7407 (1998).
[34] We calculated the band gap of 3C-SiC using the same method and found it to be only 1.6 eV, which is underestimated by about 30% compared to the experimental value of 2.4 eV. This underestimation always exists in the band gap calculations (Refs. 9 and 27), especially when the local density approximation (LDA) is used for the exchange-correlation potential, due to the limitation of DF theory. The values of band gaps are slightly improved even when the GGA is employed. However, the trend of band gap variation as a function of tube diameter and chirality, as well as the characters of band structures from calculations, is expected to be reasonable and reliable.
[35] A. Garcia and M. L. Cohen, Phys. Rev. B **47**, 4215 (1993).
[36] R. Tenne and A. K. Zettl, in *Carbon Nanotubes: Synthesis, Structure, Properties, and Applications*, edited by M. S. Dresselhaus, G. Dresselhaus, and P. Avouris (Springer, Berlin, 1996), pp. 81–111.
[37] X. Blasé, L. X. Benedict, E. L. Shirley, and S. G. Louie, Phys. Rev. Lett. **72**, 1878 (1994).
[38] S. Reich, C. Thomsen, and P. Ordejón, Phys. Rev. B **65**, 155411 (2002).